Check for updates

ADVANCED HEALTHCARE MATERIALS
www.advhealthmat.de

Microgels as Platforms for Antibody-Mediated Cytokine Scavenging

Sarah Boesveld, Yonca Kittel, Yizhao Luo, Alexander Jans, Burak Oezcifci, Matthias Bartneck, Christian Preisinger, Dirk Rommel, Tamás Haraszti, Silvia P. Centeno, Arnold J. Boersma, Laura De Laporte, Christian Trautwein,* Alexander J. C. Kuehne,* and Pavel Strnad**

Therapeutic antibodies are the key treatment option for various cytokine-mediated diseases, such as rheumatoid arthritis, psoriasis, and inflammatory bowel disease. However, systemic injection of these antibodies can cause side effects and suppress the immune system. Moreover, clearance of therapeutic antibodies from the blood is limiting their efficacy. Here, water-swollen microgels are produced with a size of 25 µm using droplet-based microfluidics. The microgels are functionalized with TNFα antibodies to locally scavenge the pro-inflammatory cytokine TNFα. Homogeneous distribution of TNFα-antibodies is shown throughout the microgel network and demonstrates specific antibody-antigen binding using confocal microscopy and FLIM-FRET measurements. Due to the large internal accessibility of the microgel network, its capacity to bind TNFα is extremely high. At a TNFα concentration of 2.5 µg mL^{-1}, the microgels are able to scavenge 88% of the cytokine. Cell culture experiments reveal the therapeutic potential of these microgels by protecting HT29 colorectal adenocarcinoma cells from TNFα toxicity and resulting in a significant reduction of COX II and IL8 production of the cells. When the microgels are incubated with stimulated human macrophages, to mimic the in vivo situation of inflammatory bowel disease, the microgels scavenge almost all TNFα that is produced by the cells.

1. Introduction

Since their introduction more than three decades ago, therapeutic antibodies have become the predominant treatment modality for various diseases, such as rheumatoid arthritis, psoriasis, Crohn´s disease, or ulcerative colitis. Consequently, many of the best-selling drugs today are monoclonal antibodies.[1] Several of these antibody drugs are designed to scavenge cytokines, such as TNFα, IL-1ß, IL-6, or IL12/23, as key inflammatory mediators and are used for treatment of different immune-mediated disorders. Among them, TNFα antibodies represent the most widely used class of antibody drugs.[1] However, its systemic administration leads to significant immunosuppression and increases the risk of serious infections and malignancies, as well as systemic inflammatory responses.[2,3] Moreover, in vivo, the antibodies encounter harsh environmental conditions, which lead to their deactivation

S. Boesveld, Y. Luo, A. Jans, M. Bartneck, C. Trautwein, P. Strnad
Department of Internal Medicine III
University Hospital
RWTH Aachen University
Pauwelsstraße 30, 52074 Aachen, Germany
E-mail: ctrautwein@ukaachen.de; pstrnad@ukaachen.de
Y. Kittel, B. Oezcifci, D. Rommel, T. Haraszti, S. P. Centeno, A. J. Boersma, L. De Laporte
DWI-Leibniz Institute for Interactive Materials
RWTH Aachen University
Forckenbeckstraße 50, 52074 Aachen, Germany
E-mail: delaporte@dwi.rwth-aachen.de

The ORCID identification number(s) for the author(s) of this article can be found under https://doi.org/10.1002/adhm.202300695

© 2023 The Authors. Advanced Healthcare Materials published by Wiley-VCH GmbH. This is an open access article under the terms of the Creative Commons Attribution-NonCommercial License, which permits use, distribution and reproduction in any medium, provided the original work is properly cited and is not used for commercial purposes.

DOI: 10.1002/adhm.202300695

Y. Kittel, D. Rommel, T. Haraszti, L. De Laporte
Institute for Technical and Macromolecular Chemistry (ITMC)
RWTH Aachen University
Worringerweg 2, 52074 Aachen, Germany
Y. Kittel, A. J. C. Kuehne
Institute of Organic and Macromolecular Chemistry
Ulm University
Albert-Einstein-Allee 11, 89081 Ulm, Germany
E-mail: alexander.kuehne@uni-ulm.de
B. Oezcifci, A. J. Boersma
Department of Cellular Protein Chemistry
Bijvoet Center for Biomolecular Research
Utrecht University
Padualaan 8, Utrecht 3584 CH, The Netherlands
C. Preisinger
Proteomics Facility
Interdisciplinary Centre for Clinical Research (IZKF)
Medical School
RWTH Aachen University
Pauwelsstraße 30, 52074 Aachen, Germany

21922659, 2023, 18, Downloaded from https://onlinelibrary.wiley.com/doi/10.1002/adhm.202300695 by Rwth Aachen Hochschulbibliothek, Wiley Online Library on [25/03/2024]. See the Terms and Conditions (https://onlinelibrary.wiley.com/terms-and-conditions) on Wiley Online Library for rules of use; OA articles are governed by the applicable Creative Commons License

and therefore require higher concentrations of the administered antibodies to retain efficacy. To increase the therapeutic efficiency, and minimize the dose and systemic side effects, the immobilization of antibodies on carriers, such as liposomes or nanoparticles, represents a promising approach.[4–6] IL-6 antibodies have been immobilized on the surface of polymeric nanoparticles to selectively capture the pro-inflammatory cytokine IL-6 in inflammatory diseases, such as arthritis.[6] Moreover, the co-immobilization of two types of monoclonal antibodies against effector and tumor cells on nanoparticles has shown therapeutic superiority, in comparison to free antibody and mono-functionalized nanoparticles in vitro and in vivo in cancer immunotherapy.[5] However, such antibody-nanoparticle conjugates often suffer from accelerated blood clearance,[7] and conjugating an antibody to a surface might sterically restrict access to the binding motif, resulting in low binding capacity and strength.[8]

To overcome these challenges, we propose to use water-swollen, soft microgels as carriers, which exhibit high internal binding capacity as well as stealth against immune recognition to evade physiological clearance.[9] As opposed to typical nanoparticle approaches, microgels exhibit an open-meshed polymer network and can therefore also be functionalized on their inside, greatly increasing the capacity of these carrier systems.[10] To date, microgels have only been employed for presenting antibodies to isolate tumor cells from the environment via cancer immunotherapy, or to scavenge NO (nitric oxide) and ROS (reactive oxygen species).[11-14] Extending these microgel functions to scavenging of cytokines would greatly enhance the spectrum of treatments for inflammatory diseases by increasing the binding performance and reducing side effects. The size and stiffness of microgels can be tuned so that they can be applied systemically or locally, while precisely controlling their ability to cross and interact with barriers,[15] such as cell membranes,[16] the intestine and mucus,[17,18] blood vessels,[19] skin,[20] and the blood-brain barrier.[21] Whereas anti-inflammatory antibodies against TNFα that are released in the intestine can still pass the intestinal barrier and enter the blood circulation,[22,23] engineered microgels with micron-scale diameters could prevent this transition.[18] Such micron-sized microgels are biocompatible, deformable, and stable against changes in pH, and cellular uptake is prevented. The route of administration will depend on the type of disease. For example, in the case of inflammatory bowel disease, a chronic intestinal disorder, oral administration would be advantageous. This would enable local therapy with subsequent excretion of the microgels. We have previously presented a microgel scavenging system that can take up and multivalently bind cholera toxin, leading to higher affinity as compared to surface receptors of HT29 intestinal cells.[24]

Here, we develop immunoglobulin G (IgG) antibody functionalized polyethylene glycol (PEG)-based microgels as scavengers for the pro-inflammatory cytokine TNFα (schematically shown in **Figure 1**C). The microgels are produced by microfluidics and have diameters of ≈ 25 µm. The IgG antibodies are conjugated to reactive glycidyl groups in the PEG-based microgels using mild glycidyl-amine coupling. Our microgel system shows high binding capability of the cytokine TNFα in a biologically relevant range.

2. Results and Discussion

2.1. Microgel Synthesis and Characterization

To prevent cellular uptake and crossing of the intestinal barrier, uniform microgels with a defined diameter in the range of the size of a cell (diameter ≈ 25 µm) are synthesized via a previously described flow-focusing microfluidic technique[24,25] (see Figure 1A,B). Monodisperse droplets are formed in the microfluidic chip using the dispersed phase consisting of an aqueous solution of star-PEG acrylate (sPEG-Ac) polymers with glycidyl methacrylate (GMA; 10 mol per mol sPEG-Ac) and Irgacure 2959 as the photo-initiator and the continuous oil phase. The collected droplets are irradiated with UV light at a wavelength of λ = 365 nm (200 mW, t = 180 s), inducing free radical polymerization and crosslinking to form the microgels. The microgels are then separated from the continuous phase, purified, and sterilized as explained in detail in the Materials and Methods section.

2.2. Diffusion Studies with Antigen- and Antibody Mimicking Dextrans

Before testing therapeutic IgG antibodies and targeted antigens, we employ dextran, labeled with fluorescein isothiocyanate (FITC), with a molecular weight of 20 kDa and a hydrodynamic radius (R_h) of ≈ 3.3 nm to mimic TNFα ($R_h = 3.2 \pm 0.04$ nm),[26] and a second set of fluorescently labeled dextran with molecular weight of 70 kDa ($R_h \approx 6.0$ nm) to mimic the IgG antibody ($R_h = 5.6 \pm 0.24$ nm).[26] The latter has an amine functionality that is able to bind to the glycidyl-groups introduced via the GMA comonomer and functions as a proof-of-concept molecule to examine the accessibility, reactivity, and ability of our microgels to take up and bind macromolecules. In a first step, diffusion of the FITC dextran (M_n = 20 kDa) is analyzed inside microgels prepared from various PEG compositions and 10 equivalents (eq.) of GMA per sPEG-Ac to investigate the impact of the crosslink density of the polymer network on the diffusion coefficient D. Therefore, we synthesize microgels with four- or eight-armed sPEG-Ac and different molecular weights of 10, 20, or 40 kDa at varying ratios and determine the diffusion coefficient using fluorescence recovery after photobleaching (FRAP) method (see Figure 1A,E). For all microgels, the diffusion coefficient is around $D = 15$ µm^2 s^{-1} and thus not affected by the different microgel networks. Sequentially, we monitor diffusion of the larger fluorescein amine dextran (M_n = 70 kDa) into the same microgels after 96 h incubation time at a theoretical molar ratio dextran:GMA of 1 by confocal laser-scanning microscopy (CLSM) (see Figure 1F; Figure S1, Supporting Information). Similar as for the small 20 kDa FITC dextran, no differences in diffusion are observed for the different microgels. Based on the diffusion coefficients and the Ogston

L. De Laporte
Advanced Materials for Biomedicine (AMB), Institute of Applied Medical Engineering (AME) Department of Center for Biohybrid Medical Systems (CBMS)
Forckenbeckstraße 55, 52074 Aachen, Germany

© 2023 The Authors. Advanced Healthcare Materials published by Wiley-VCH GmbH

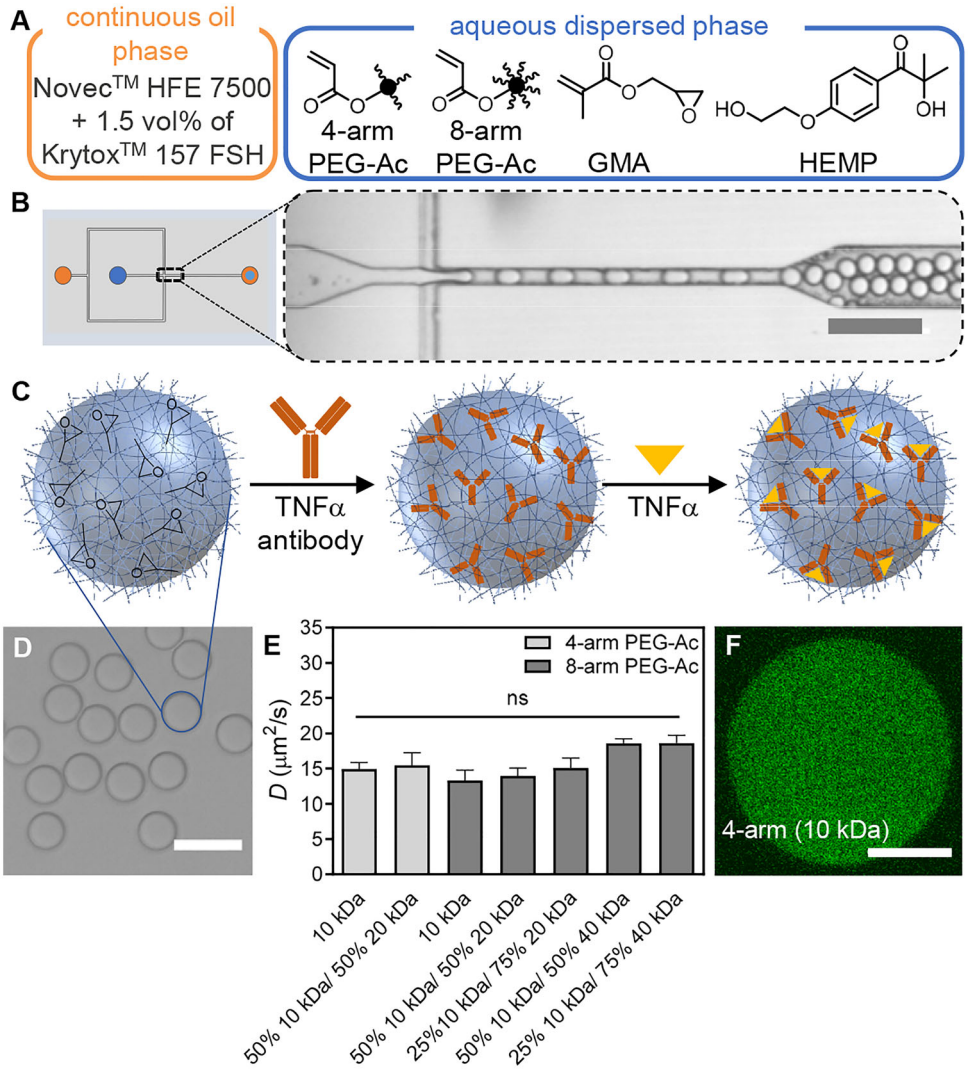

Figure 1. A) Composition of continuous and aqueous dispersed phases used in microfluidics. Continuous phase consists of Novec HFE 7500 (a fluorinated ether) with 1.5 vol% of Krytox H as a stabilizing agent, while glycidyl methacrylate (GMA) and 2-Hydroxy-4′-(2-hydroxyethoxy)-2-methylpropiophenone (HEMP, also known as Irgacure 2959) is added to the aqueous phase. B) Microfluidic set-up for the production of spherical microgels with different sPEG-Ac polymers at a total concentration of 10 wt%. C) Schematic representation of TNFα scavenging microgels:glycidyl-co-polymerized PEG microgels are post-functionalization with TNFα antibodies to scavenge TNFα. D) Brightfield image of collected and purified microgels (10 wt% 4-arm PEG-Ac (10 kDa, 10 eq. GMA)) in water. The scale bar represents 50 μm. E) Diffusion coefficients D of fluorescein isothiocyanate (FITC) dextran (20 kDa) in microgels with different polymer compositions and 10 eq. GMA was determined via FRAP technique. Data are shown as mean ± standard deviation, $n = 5$ microgels. Statistical significance is performed using two-way ANOVA with Tukey´s test for multiple comparisons: ns = non-significant. F) Confocal laser-scanning microscopy (CLSM) images of the diffusion of fluorescein amine dextran (70 kDa) into microgels (10 wt% 4-arm PEG-Ac (10 kDa, 10 eq. GMA)) after 96 h of incubation. Scale bars represent 10 μm.

expression,[27] the average mesh size is estimated to be between ca. 6.1 and 8.8 nm for all microgel conditions, which is larger than the hydrodynamic diameter of the antibody mimicking dextran ($M_n = 70$ kDa, ≈ 6 nm) (see Table S1 and Figure S3, Supporting Information). We used this obstruction model (as described in the method section), which is based on the premise that solute movement through the microgel network is impeded by the polymer chains.[27] Importantly, the microgels produced with 4-arm sPEG-Ac (10 kDa) are the most stable and do not aggregate compared to the other microgel conditions (see Figure 1D; Figure S2, Supporting Information). Therefore, this composition is selected for the continuation of this study. Microgel aggregation can occur due to increasing hydrophobicity by increasing the number of acrylate groups by changing the number of arms and molecular weight of the used sPEG-Ac. With increasing hydrophobicity, the microgels behave more like solid particles, so elevated attraction forces may be induced.[28]

To further assess the immobilization efficiency of our functional microgels via amine/glycidyl addition, we incubate microgels made with 4-arm sPEG-Ac (10 kDa) and 10 eq. of GMA per sPEG-Ac with fluorescein amine dextran (M_n = 70 kDa) for 2, 4, 8, and 16 days and measure the level of their fluorescence via

© 2023 The Authors. Advanced Healthcare Materials published by Wiley-VCH GmbH

21922659, 2023, 18, Downloaded from https://onlinelibrary.wiley.com/doi/10.1002/adhm.202300695 by Rwth Aachen Hochschulbibliothek, Wiley Online Library on [25/03/2024]. See the Terms and Conditions (https://onlinelibrary.wiley.com/terms-and-conditions) on Wiley Online Library for rules of use; OA articles are governed by the applicable Creative Commons License

21922659, 2023, 18, Downloaded from https://onlinelibrary.wiley.com/doi/10.1002/adhm.202300695 by Rwth Aachen Hochschulbibliothek, Wiley Online Library on [25/03/2024]. See the Terms and Conditions (https://onlinelibrary.wiley.com/terms-and-conditions) on Wiley Online Library for rules of use; OA articles are governed by the applicable Creative Commons License

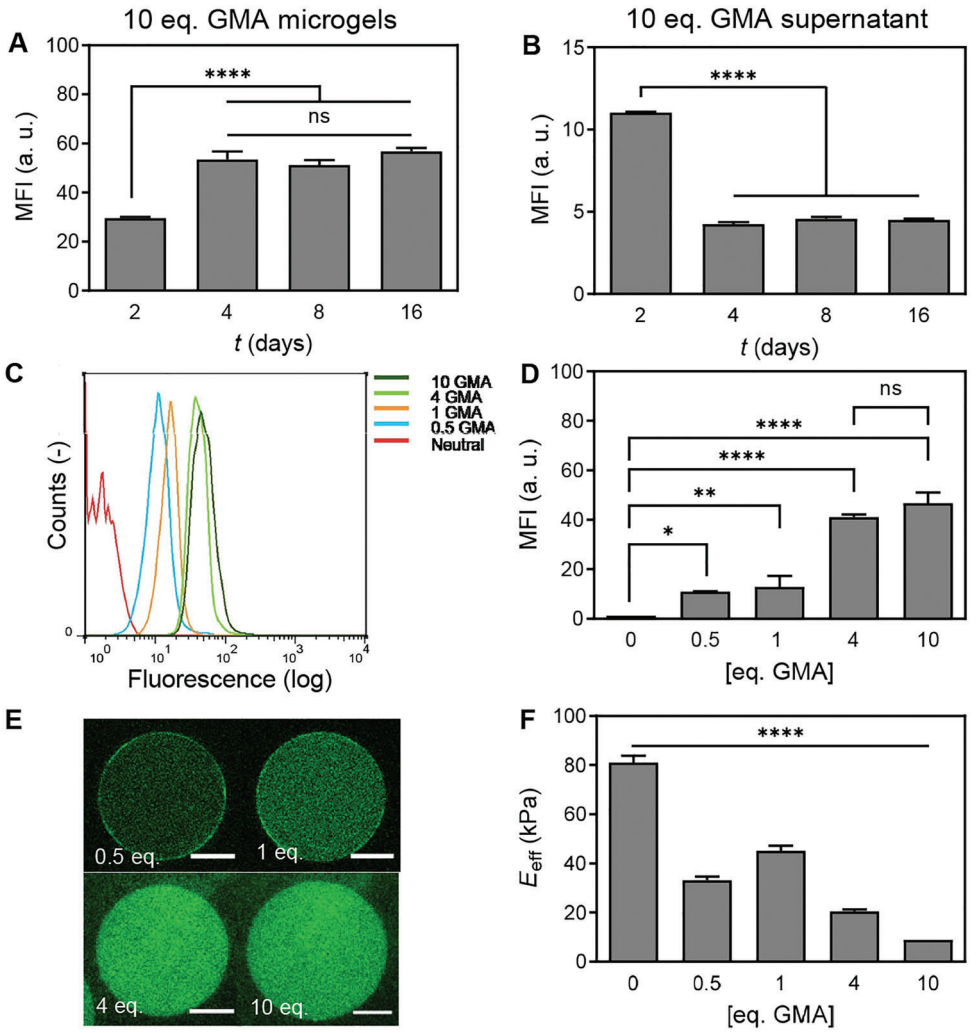

Figure 2. Time-dependent binding of fluorescein amine dextran to GMA functionalized microgels (10 wt% 4-arm sPEG-Ac (10 kDa). A) Flow cytometry-based mean fluorescence intensity (MFI) of microgels (10 eq. GMA) incubated with fluorescein amine dextran (70 kDa) for 2, 4, 8. and 16 days. B) Measurements of fluorescence in corresponding supernatant via plate reader. C) Flow cytometry plots of microgels containing increasing amounts of GMA ranging from 0.5 to 10 eq. that are incubated with fluorescein amine dextran for 4 days. D) Corresponding plot of the mean fluorescence intensity (MFI) shown in (C), $n \geq 3$. E) Confocal images of microgels containing different amounts of GMA (0.5, 1, 4, and 10 eq.) that are incubated with fluorescein amine dextran (70 kDa) for 4 days. Scale bars represent 10 µm. F) Effective Young's modulus (E_{eff}) of microgels containing different eq. of GMA determined via nanoindentation; $n \geq 10$ microgels. Data are presented as mean ± standard deviation. Statistical significance is performed using two-way ANOVA with Tukey´s test for multiple comparisons: ns = non-significant; $^{*}p < 0.05$, $^{**}p < 0.01$, $^{****}p < 0.0001$.

flow cytometry. After 4 days of incubation, saturation is reached as verified by investigating the fluorescence of the supernatant, (see **Figure 2**A). The fluorescence in the supernatant does not decrease significantly after 4 days of incubation, meaning that the microgels have reached their uptake limit (see Figure 2B).

2.3. Optimization of GMA Concentration Inside the Microgels

To investigate the required amount of GMA inside the microgels to link a maximum number of antigen-binding sites inside the microgel, we vary the GMA concentration during synthesis. Therefore, we synthesize microgels with 0.5, 1, 4, or 10 eq. GMA per sPEG-Ac and incubate them over the course of 4 days with a stoichiometric concentration of fluorescently labeled amine dextran (dextran:GMA of 1). The fluorescence intensity is analyzed using flow cytometry analysis and CLSM (see Figure 2C–E). While a significant augmentation of dextran binding is observed for an increase from 1 to 4 eq. of GMA, no further differences are observed in the fluorescence signal between microgels made with 4 and 10 eq. GMA (see Figure 2C–E). Microgels without copolymerized GMA show only negligible fluorescence, indicating minimal unspecific binding to the fluorescein amine dextrans. Importantly, the incorporation of more or less GMA will affect the network morphology, as it separates the sites for crosslinking and increases the mesh size – at least before any binding motifs are attached to the glycidyl units. This is confirmed by the increased stiffness for the lower GMA concentrations of 0.5 and 1 eq. (see Figure 2F), suggesting a smaller mesh size. To analyze this, FRAP experiments on the micro-

 © 2023 The Authors. Advanced Healthcare Materials published by Wiley-VCH GmbH

21922659, 2023, 18, Downloaded from https://onlinelibrary.wiley.com/doi/10.1002/adhm.202300695 by Rwth Aachen Hochschulbibliothek, Wiley Online Library on [25/03/2024]. See the Terms and Conditions (https://onlinelibrary.wiley.com/terms-and-conditions) on Wiley Online Library for rules of use; OA articles are governed by the applicable Creative Commons License

gels with different GMA concentrations are performed with FITC dextran (M_n = 20 kDa), mimicking the size of the antigen (see Figure S4, Supporting Information). Only in the case of 4 and 10 eq. GMA microgels (10 wt% 4-arm PEG-Ac (10 kDa)), we were able to measure a diffusion coefficient of 7.4 and 18.3 $\mu m^2\ s^{-1}$, respectively. In the case of 0.5 and 1 eq., FITC dextran (M_n = 20 kDa) did not diffuse (see Figure S4, Supporting Information) into the microgels as the mesh size becomes too small. Furthermore, to study the effect of increasing mesh size with increasing GMA, we determine Young's modulus via nanoindentation on isolated microgels immobilized on a surface. As expected, microgels with higher GMA concentrations are softer than those with no or low concentrations of GMA (see Figure 2F). Notably, such a decrease in stiffness has previously also been reported for introducing amine methacrylate as a co-monomer in microfluidically produced sPEG-Ac microgels.[29] Microgel stiffness and deformability are important when interacting with biological interfaces. PEG-based rod-shaped microgels with an effective Young's modulus of ≈ 20 kPa, modified with RGD, supported cell attachment, spreading, and growth when incubated with human fibroblasts and HUVECs.[29] Moreover, sPEG-based spherical microgels were assembled into microporous tissue scaffolds, while scaffolds with a storage modulus of 13.5 kPa showed best cell proliferation when incubated with human fibroblasts.[30] These stiffnesses are comparable to our microgels made from 10 wt% 4-arm sPEG-Ac (10 kDa) and a GMA amount of 10 and 4 eq.

After demonstrating homogeneous uptake and binding of the dextran as an IgG antibody-mimicking molecule, we investigate whether a second molecule could still diffuse through the polymer network after the first functionalization. In the real system, TNFα would need to diffuse through the network and bind to the IgG antibody. To mimic TNFα, we incubate the 70 kDa dextran-coupled microgels (10 eq. GMA, 4-arm sPEG-Ac (10 kDa)) with a second dextran (M_n = 20 kDa) labeled with red fluorescent Rhodamine B, at a concentration of dextran:GMA of 1 over a course of 96 h. Analysis via CLSM shows homogeneously green (before) and red-fluorescing microgels (after incubation), indicating that a small molecule like TNFα will be able to diffuse and bind into the microgel network after coupling the IgG (see Figure S5, Supporting Information).

2.4. Antibody Binding Inside the Microgels

Based on our binding efficiency experiments, we consider microgels with 4 or 10 eq. GMA as most suitable to function as antigen scavengers as they showed significantly higher fluorescence intensity compared to lower eq. GMA. Therefore, microgels (10 wt% 4-arm sPEG-Ac (10 kDa)) with 4 and 10 eq. are incubated with IgG antibodies for 4 days to quantify uptake and binding to the microgel network via amine-glycidyl addition. After purification of the microgels, we analyze the bound protein content with a CBQCA protein quantification kit. It becomes clear that for both types of microgels, the level of bound IgG antibody increases with higher amounts of incubated antibody. Interestingly, microgels with 10 eq. GMA bind significantly more IgG antibody compared to microgels with 4 eq. GMA, although this difference is not observed in the binding study with fluorescently labeled amine dextran of 70 kDa (see Figures 2C–E and **3**), could be related to fluorescence quenching. For the quantitative protein assay, different molar ratios of IgG:GMA, ranging from 0.01 to 1, are tested. In the case of IgG:GMA = 0.1 for 4 eq. GMA in the microgels, a concentration of bound IgG [IgG] = 191.62 ± 4.1 µg of IgG/10^5 microgels (µGs) is observed, while for 10 eq. GMA in the microgels, [IgG] = 330 ± 6.6 µg/10^5 µGs. When we increase the IgG concentration during incubation, we see that the amount of bound antibody increases proportionally up to the theoretical stoichiometric ratio of IgG:GMA = 1, demonstrating that IgG can easily reach and react with the glycidyl groups. However, it is also clear that most IgG remains in the supernatant and does not bind to the microgels. This is expected as ≈100 000 microgels (total volume of ≈ 400 µL) are incubated in a volume of 1200 µL containing the IgG. Based on these results, microgels made with 10 eq. GMA is selected for the continuation of the study. In order to decouple microgel stiffness with the antibody conjugation, quenching of free glycidyl groups to simulate less antigen binding sites in the 10 eq. GMA microgels will be performed in future experiments.

2.5. Specific Antibody-Antigen Binding Inside the Microgels

First, in order to ensure that the antibody is still active after binding to the microgels, we investigate different methods to bind the antibody to the GMA-equipped microgels without losing its activity. The microgels are functionalized with the antibody directly, with Protein A and in a second step with the antibody, or with a Protein A-antibody complex (see Figure S6, Supporting Information). From these results, it is clear that direct coupling of the antibody to GMA in the microgels is the most efficient. To investigate whether TNFα can diffuse and bind to the antibody functionalized microgels, we incubate either ≈100 000 non-functionalized or functionalized microgels with two different TNFα concentrations, 0.5 µg mL^{-1} ($2.9 \cdot 10^{-8}$ mol mL^{-1}) (see **Figure 4**A) and 2.5 µg mL^{-1} ($1.5 \cdot 10^{-7}$ mol mL^{-1}) (see Figure 4B), in a volume of 500 µL and analyze the supernatant via ELISA. Even though non-functionalized microgels behave like sponges and absorb approximately half of the applied TNFα when using a concentration of 0.5 µg mL^{-1}, functionalized microgels with IgG:GMA = 0.01 scavenge significantly more TNFα compared to non-functionalized microgels (see Figure 4A). Increasing the IgG:GMA ratio further increases the scavenging potential, showing complete uptake at a ratio of 0.05 for an applied concentration of 0.5 µg mL^{-1} TNFα (see Figure 4A). This experiment shows that at low [TNFα] = 0.5 µg mL^{-1}, microgels with IgG:GMA = 0.05 scavenge virtually all TNFα and are as efficient as for the case of stoichiometric functionalization. To further test the limits of the microgels to scavenge TNFα, the same microgels are incubated with a fivefold higher concentration of [TNFα] = 2.5 µg mL^{-1} (see Figure 4B). Here, it requires microgels with a stoichiometric IgG:GMA ratio of 1 to be able to scavenge 88% of the applied TNFα. Moreover, for microgels with a theoretical IgG:GMA ratio of 0.1, ≈ 50% of the applied TNFα is scavenged, when incubated with [TNFα] = 2.5 µg mL^{-1}.

Importantly, both tested TNFα concentrations are far beyond the disease-relevant levels. For example, the TNFα concentration in the intestinal tissue during an acute dextran sodium sulfate (DSS) induced colitis in mice has been reported to be in the

© 2023 The Authors. Advanced Healthcare Materials published by Wiley-VCH GmbH

21922659, 2023, 18, Downloaded from https://onlinelibrary.wiley.com/doi/10.1002/adhm.202300695 by Rwth Aachen Hochschulbibliothek, Wiley Online Library on [25/03/2024]. See the Terms and Conditions (https://onlinelibrary.wiley.com/terms-and-conditions) on Wiley Online Library for rules of use; OA articles are governed by the applicable Creative Commons License

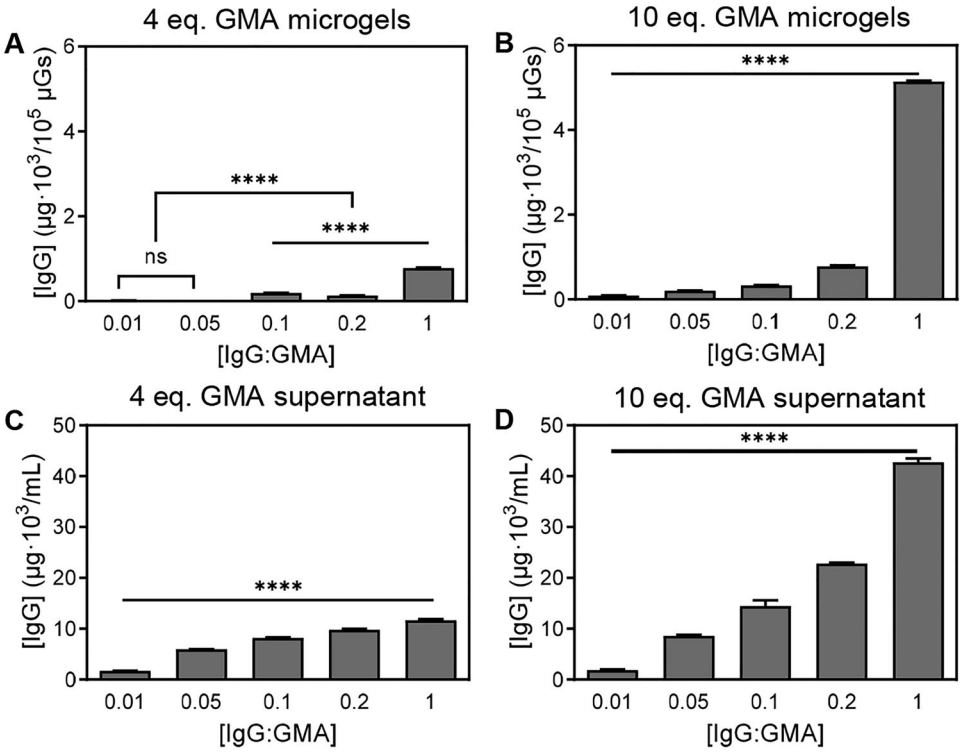

Figure 3. Functionalization of microgels (10 wt% 4-arm sPEG-Ac (10 kDa, 4 and 10 eq. GMA)) with IgG antibody against human TNFα. The concentration of antibodies in microgels prepared with 4 (A) and 10 (B) eq. of GMA, as well as in the corresponding supernatants (C,D) is measured via a CBQCA protein quantification kit. Data are presented as mean ± standard deviation, $n = 3$. Statistical significance is performed using two-way ANOVA with Tukey´s test for multiple comparisons: ns = non-significant; $^{****}p < 0.0001$.

pg mL^{-1} range.[31,32] For this reason, the following experiments are performed using microgels with IgG:GMA = 0.1, as this ratio is adequate to incorporate sufficient antibodies with respect to physiological levels of TNFα and will allow for ample binding to scavenge the antigen in cytokine-mediated diseases. At this ratio, we can nearly completely remove TNFα up to concentrations of 0.5 µg mL^{-1}, which is still far above the physiological concentration (see Figure 4C).

Unfortunately, we are not able to calculate or estimate a dissociation constant for the antibody in the microgels as we already went up to a level of TNFα, which exceeds the physiological concentration range by far and still we do not reach saturation of the microgels, which would be required to estimate or determine an uptake efficiency.

To further quantify how efficiently TNFα diffuses into and binds to the antibody functionalized microgels (10 eq. GMA, 0.1 IgG:GMA), we label the antibody (IgG) inside of the microgels with Alexa Fluor 546 (AF546) and the TNFα antigen with Alexa Fluor 488 (AF488). These two dyes can engage in Förster resonance energy transfer (FRET) and therefore represent a FRET pair, with the antibody functioning as the FRET acceptor and TNFα as the donor. First, we incubate microgels without the FRET donor with the fluorescently labeled antibody and we observe fluorescence emission (represented in purple) inside the microgels after washing and excitation at 561 nm (see **Figure 5**A,B). This corroborates that the functionalization with the fluorescently labeled antibody is successful. Second, we image the fluorescently labeled TNFα inside of the microgels in absence of the FRET acceptor IgG resulting in a homogeneous fluorescence emission after excitation at 488 nm (represented in yellow) (see Figure 5C). After this, the fluorescently labeled TNFα FRET donor is incubated at 138 µg mL^{-1} with ≈50 000 microgels carrying the FRET acceptor functionalized antibodies. When we excite only with the 488 nm laser line, we observe fluorescence of AF488 in the donor channel (yellow) and in addition the fluorescence of AF546 in the acceptor channel (purple), which indicates that the Förster energy transfer is efficient, and we can therefore infer that the TNFα is binding specifically to the TNFα antibodies (see Figure 5D).

However, to confirm FRET[33] as the origin for the acceptor emission, we performed additional Fluorescence Lifetime Imaging (FLIM)[34] measurements of 10 different microgels. In the FLIM experiments, we excite also with the 488 nm laser line but collect only the fluorescence of the donor. In addition to the number of photons, we can resolve the kinetics of the fluorescence emission. By looking at the lifetime of the fluorescence decay, we can detect the FRET process, since in such a case the lifetime of the donor is shortened, due to the additional FRET deactivation channel. Indeed, we observe a shift of the lifetime of the donor labeled TNFα (see fluorescence lifetime image in Figure 5F and schematically shown in Figure 5I) from, ≈ 4.02 ± 0.02 ns in solution (see Figure 5M) to a value of 3.01 ± 0.09 ns (see Figure 5M), (intensity averaged lifetime), confirming the FRET interaction (see fluorescence lifetime image in Figure 5H and schematically shown in Figure 5K; Figure S7, and Tables S2–S6, Supporting Information). However, we also observe some quenching of the

© 2023 The Authors. Advanced Healthcare Materials published by Wiley-VCH GmbH

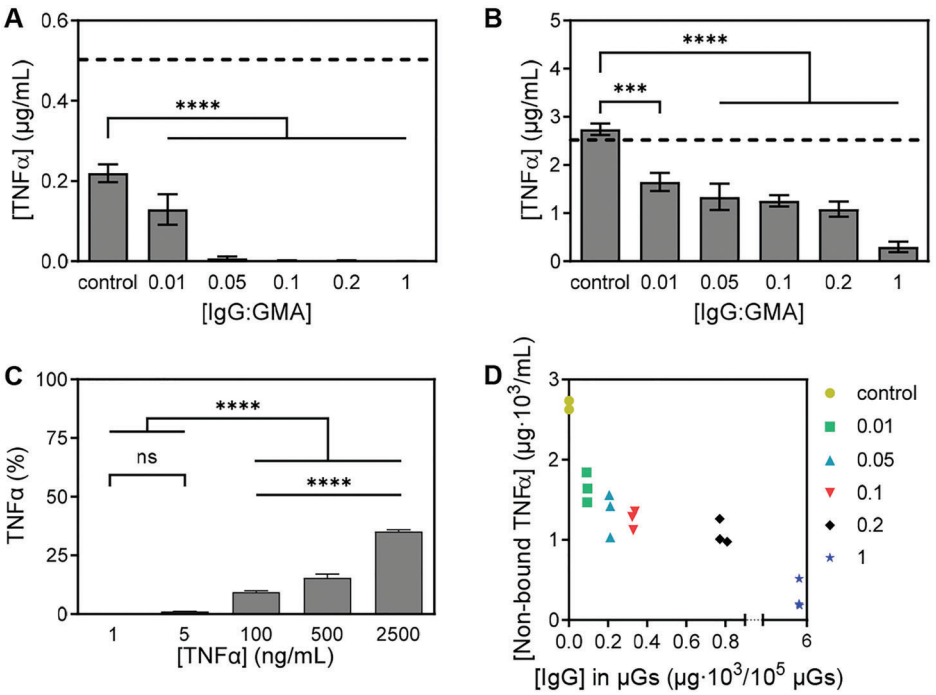

Figure 4. TNFα binding to microgels (10 wt% 4-arm sPEG-Ac (10 kDa, 10 eq. GMA)) ([microgels] = 200 000 microgels mL^{-1} = 100 μg mL^{-1}). A) 0.5 μg mL^{-1} TNFα is incubated with microgels containing different glycidyl-antibody ratios [IgG:GMA]. Non-bound TNFα is measured in the supernatant via TNFα ELISA. B) 2.5 μg mL^{-1} TNFα is incubated with microgels containing different glycidyl-antibody ratios [IgG:GMA]. Non-bound TNFα is measured in the supernatant via TNFα ELISA. C) Antibody-functionalized microgels (IgG:GMA = 0.1) are incubated with increasing concentrations of TNFα. Non-bound TNFα is measured in the supernatant via TNFα ELISA and shown as a percentage. D) Shows the correlation between the amount of incorporated antibody and scavenged TNFα for a fixed concentration of 2.5 μg mL^{-1} TNFα. Data are presented as mean ± standard deviation, $n = 3$. Statistical significance is performed using two-way ANOVA with Tukey´s test for multiple comparisons: ns = non-significant, $^{***}p < 0.001$, $^{****}p < 0.0001$.

donor lifetime to a value of ≈ 3.61 ± 0.09 ns (intensity averaged lifetime) (see Figure 5M) when donor labeled TNFα is freely diffusing in the microgels without the antibody-acceptor moiety (see Figures 5G and schematically shown in Figure 5J). Unfortunately, this quenching, which is observed as a multiexponential decay (Tables S3 and S4, Supporting Information), prevents us from being able to quantify the cytokine/antibody binding with fidelity. The origin of the non-FRET quenching was not further investigated in this work but is likely caused by interaction with the microgel network. Further studies are needed to determine whether the binding of the antibody to the microgels reduces its efficiency, potentially by surface plasmon resonance.

2.6. Microgels Protect HT29 Cells from TNFα Induced Inflammation

Our optimized microgels for TNFα scavenging are now tested in their ability to protect HT29 colorectal adenocarcinoma cells from cytokine toxicity. We perform a competition experiment, where HT29 cells are exposed to TNFα and microgels (antibody functionalized and non-functionalized) at the same time. The levels of COX II and the release of IL8 or LDH into the cell culture medium are used as indicators for TNFα toxicity.[35,36] Exposing the cells to TNFα at a concentration of 5 ng mL^{-1} is sufficient to induce the biosynthesis of COX II, as well as the release of IL8 and LDH into the supernatant (see Figure S9A–D, Supporting Information). The presence of a robust inflammation upon stimulation with TNFα is confirmed by increased mRNA expression of the pro-inflammatory cytokines TNFα and IL8 (see Figure S9E,F, Supporting Information). To test the scavenging function of the microgels, HT29 cells are simultaneously exposed to 5 ng mL^{-1} TNFα and either 100 μg mL^{-1} of antibody-functionalized or non-functionalized microgels, which are ≈200 000 microgels mL^{-1}. Compared to treatment with TNFα alone, the co-incubation with antibody-functionalized microgels significantly reduced COX II levels, as well as the amount of the pro-inflammatory cytokine IL8 in the cell culture supernatant (see **Figure 6**A,B). These results suggest that TNFα has a higher affinity to antibody-functionalized microgels than the corresponding receptors present on the cell surface. Importantly, non-functionalized microgels do not show this reduction in inflammatory markers. Exposure of the cells to either antibody-functionalized or non-functionalized microgels without TNFα does not induce any inflammatory or toxic effects, indicating that the microgels themselves are biocompatible (not shown).

2.7. Microgels Scavenge TNFα Produced by Human Macrophages

To achieve a supraphysiological cytokine burst, human macrophages are stimulated with lipopolysaccharide (LPS)

© 2023 The Authors. Advanced Healthcare Materials published by Wiley-VCH GmbH

21922659, 2023, 18, Downloaded from https://onlinelibrary.wiley.com/doi/10.1002/adhm.202300695 by Rwth Aachen Hochschulbibliothek, Wiley Online Library on [25/03/2024]. See the Terms and Conditions (https://onlinelibrary.wiley.com/terms-and-conditions) on Wiley Online Library for rules of use; OA articles are governed by the applicable Creative Commons License

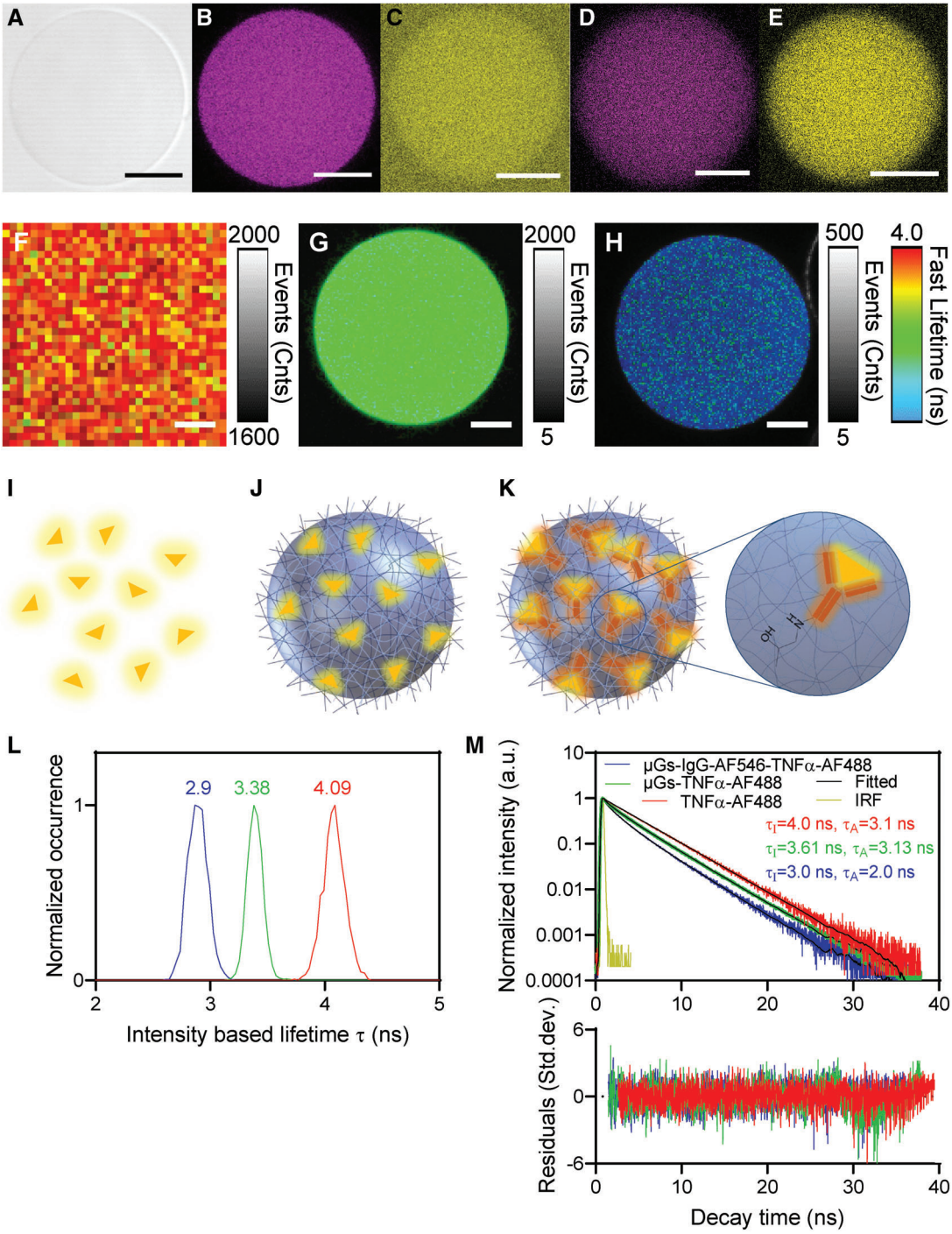

Figure 5. Specific TNFα binding to TNFα antibody-functionalized microgels ([microgels] = 50 000 microgels mL^{-1}). Confocal images of microgels (10 wt% 4-arm sPEG-Ac (10 kDa, 10 eq. GMA)) to show FRET signal. A) Brightfield image, B) TNFα antibody (acceptor, Alexa Fluor 546) functionalized microgels are excited (λ = 561 nm) and detected (λ = 571–700 nm) at acceptor wavelength. C) TNFα (donor, Alexa Fluor 488) incubated with non-functionalized microgels are excited (λ = 488 nm) and detected (λ = 498–540 nm) at donor wavelength, and D) FRET signal: TNFα antibody (acceptor) functionalized microgels incubated with TNFα (donor) are excited at donor excitation wavelength (λ = 488 nm) and detected (λ = 571–700 nm) at acceptor wavelength. E) TNFα antibody (acceptor) functionalized microgels incubated with TNFα (donor) are excited at donor excitation wavelength (λ = 488 nm) and detected (λ = 498–540 nm) at donor wavelength. Fluorescence lifetime images (FLIM) of F) only donor in solution, G) non-functionalized microgels incubated with donor, and H) TNFα antibody (acceptor) functionalized microgels incubated with donor (FRET sample). All scale bars represent 10 μm. I) Schematic of only donor in solution, J) Schematic of non-functionalized microgels incubated with donor, and K) Schematic of TNFα antibody (acceptor) functionalized microgels incubated with donor (FRET sample). L) Lifetime histograms from the FLIM images (F) (red curve), (G) (green curve), and (H) (blue curve). M) The fluorescence decays and respective exponential fittings correspond to the FLIM images (F–H).

© 2023 The Authors. Advanced Healthcare Materials published by Wiley-VCH GmbH

21922659, 2023, 18, Downloaded from https://onlinelibrary.wiley.com/doi/10.1002/adhm.202300695 by Rwth Aachen Hochschulbibliothek, Wiley Online Library on [25/03/2024]. See the Terms and Conditions (https://onlinelibrary.wiley.com/terms-and-conditions) on Wiley Online Library for rules of use; OA articles are governed by the applicable Creative Commons License

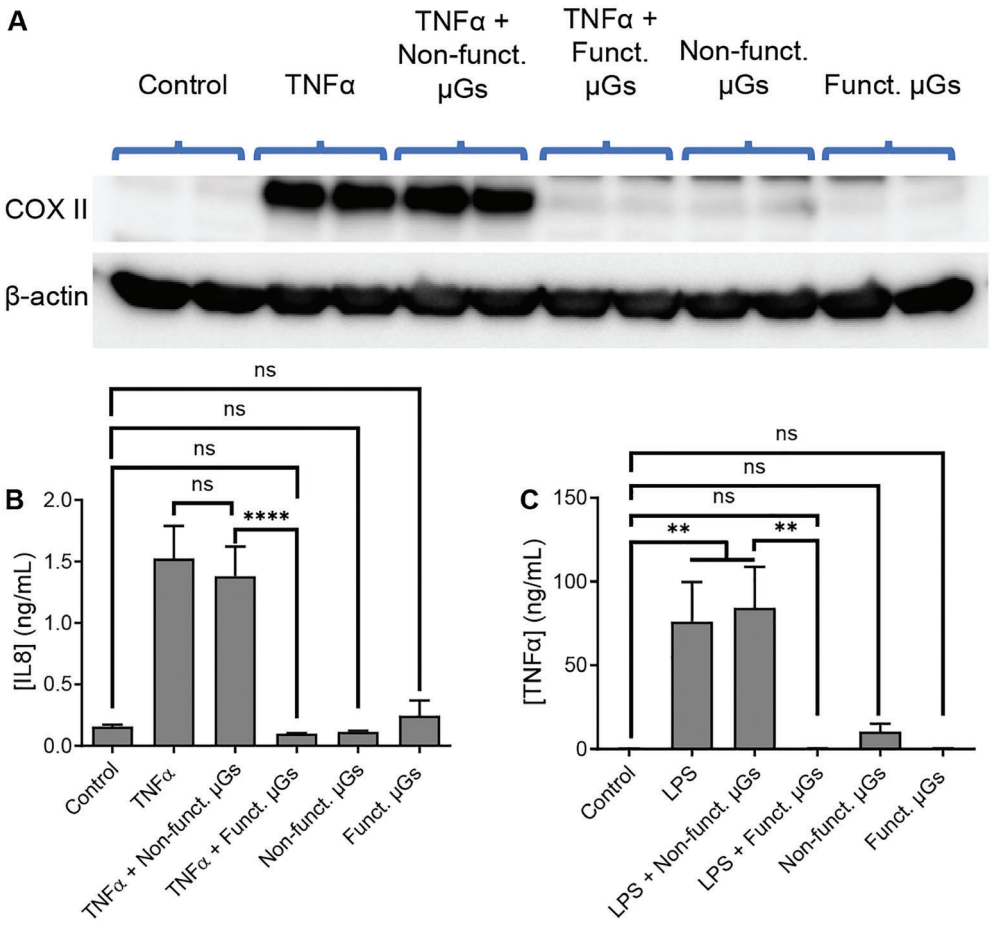

Figure 6. Microgels efficiently scavenge TNFα in two different cellular models. A,B) TNFα antibody-functionalized microgels protect HT29 cells from TNFα induced cyclooxygenase II (COX II) production, as well as interleukin 8 (IL8) release into the cell culture supernatant. Cells are exposed with 5 ng mL^{-1} TNFα alone, with TNFα together with 100 µg mL^{-1} of antibody-functionalized or non-functionalized microgels, or with microgels only for 24 h. (A) shows a COX-II western blot of protein lysates of harvested cells. ß-actin is used as a loading control. B) IL8 concentration in the cell culture supernatant is measured after incubation for 24 h. Data are presented as mean ± standard deviation, $n = 3$. Statistical significance is performed using two-way ANOVA with Tukey´s test for multiple comparisons: ns = non-significant, $^{****}p < 0.0001$. C) TNFα antibody-functionalized microgels scavenge TNFα produced by human macrophages upon stimulation with lipopolysaccharide (LPS) ($n = 5$ donors). Macrophages are stimulated with 100 ng mL^{-1} LPS, LPS, and either antibody-functionalized or non-functionalized microgels, or microgels only for 24 h. As a negative control, the cells are treated with a normal cell culture medium. The graph shows the levels of TNFα in the cell culture supernatant of the different groups. Data are presented as mean ± standard deviation, $n = 5$. Statistical significance is performed using two-way ANOVA with Tukey´s test for multiple comparisons: ns = non-significant, $^{**}p < 0.01$.

to induce the production of TNFα instead of administering TNFα to the media.[37,38] This stimulation leads to the release of ≈ 60 ng mL^{-1} of TNFα into the cell culture supernatant. Co-incubation of activated macrophages with non-functionalized microgels produces the same level of TNFα release (see Figure 6C). By contrast, co-incubation with TNFα antibody-functionalized microgels depletes TNFα virtually completely in the cell culture supernatant demonstrating their ability to scavenge the produced TNFα in real-time. Notably, co-incubation of human macrophages (no LPS activation) with non-functionalized or antibody-coupled microgels alone triggers no or only minimal TNFα production (see Figure 6C). These results suggest that microgels themselves neither activate the macrophages nor induce inflammation, which demonstrates their biocompatibility.

3. Conclusion

In summary, we show that microgels are able to bind large amounts of antibodies, which are able to efficiently scavenge pro-inflammatory antigens, in this case, TNFα. We optimized the microgels' chemical composition to incorporate large amounts of antibodies but also determined the minimal required antibody concentration inside the microgels to scavenge sufficient cytokines. Our microgels constitute an attractive approach to locally bind antigens as a treatment of cytokine-mediated inflammatory diseases. Our concept for local scavenging can be transferred and potentially be applied to various diseases, such as inflammatory bowel disease or rheumatoid arthritis, which are conventionally treated by systemic injection of therapeutic antibodies. In the next step, we plan to establish an inflammatory bowel

© 2023 The Authors. Advanced Healthcare Materials published by Wiley-VCH GmbH

21922659, 2023, 18, Downloaded from https://onlinelibrary.wiley.com/doi/10.1002/adhm.202300695 by Rwth Aachen Hochschulbibliothek, Wiley Online Library on [25/03/2024]. See the Terms and Conditions (https://onlinelibrary.wiley.com/terms-and-conditions) on Wiley Online Library for rules of use; OA articles are governed by the applicable Creative Commons License

disease animal model to test the efficacy of the antibody functionalized microgels in vivo.

4. Experimental Section

Preparation of PDMS-Based Microfluidic Devices: Microfluidic chips were used for the production of microfluidic devices via soft lithography. Sylgard 184 silicone elastomer (PDMS) and curing agent were mixed in a ratio of 10:1 in a plastic cup for 5 min. The mixture was placed in a desiccator under vacuum (10^{-3} mbar) to remove entrapped air. It was subsequently casted into the form and the air was evacuated again in the desiccator. The PDMS was cured in the oven for 12 h at 60 °C. The cured PDMS was cut out and holes for inlets and outlets in the channels were punched (biopsy puncher, inner diameter 0.75 mm). The PDMS form was washed three times with iso-propanol and water. A glass slide (76 x 52 x 1 mm, Marienfeld, Germany) was rinsed three times with acetone, iso-propanol, and water. For bonding, the PDMS replica and glass slide were activated in an oxygen plasma oven (PVA TePla 100E, Germany, Wettenberg) at an oxygen flow of 30 mL min^{-1} for 40 s at 100 W. The PDMS replica was bonded to the glass slide with the structured side and baked in the oven for 3 h at 60 °C for complete adhesion.

A hydrophobic surface coating inside of the microfluidic device channels was achieved by silanization with Tridecafluoro-1,1,2,2-tetrahydrooctyl-trichlorosilane. To enable that, the microfluidic device was positioned in a desiccator together with the silane and evacuated overnight. NovecTM HFE 7500 with 1.5 vol% of KrytoxTM 157 FSH surfactant was used to remove remaining residues of the silane from the microfluidic device.

Microgel Synthesis: A mixture of NovecTM HFE 7500 and 1.5 vol% of KrytoxTM 157 FSH surfactant was served as continuous oil phase for microgel synthesis. The dispersed aqueous phase was prepared by dissolving PEG acrylate (10 wt%) in water (HPLC gradient grade). GMA was added at a desired concentration and stirred until a homogenous solution was obtained. The radical photoinitiator 2-hydroxy-4'-(2-hydroxyethoxy)-2-methylpropiophenone (HEMP/Irgacure 2959) (0.6 wt%) was subsequently added to the solution. The vial was wrapped with aluminum foil to protect it against light-initiated polymerization.

For microfluidic synthesis of droplet-based microgels, the continuous oil and dispersed aqueous phases were each placed in a pressure vessel. The solutions were connected to the microfluidic device via PE tubing (0.38 mm ID/1.09 mm OD). The continuous oil phase consists of Novec HFE 7500 (a fluorinated ether) with 1.5 vol% of Krytox H as a stabilizing agent and the dispersed aqueous solution was prepared by mixing an aqueous solution of star-PEG acrylate (sPEG-Ac) polymers with glycidyl methacrylate (GMA; 10 mol per mol sPEG-Ac) and Irgacure 2959 as the photo-initiator. The applied pressures for droplet generation for the continuous oil phase and the dispersed aqueous solutions were 220 and 260 mbar, respectively. The produced monodisperse droplets were left out of the microfluidic device via PE tubing in the outlet channel. The tubing was irradiated with UV light (λ_{max} = 365 nm, 200 mW, t = 180 s) to polymerize the droplets via free radical polymerization. The microgels were collected in an Eppendorf vial filled with continuous oil phases to prevent them from drying out. The microgels were stored at 4 °C until purification.

Prior to purification, the continuous oil phase and an aqueous phase containing microgels formed a two-phase system. First, the oil phase was removed using a syringe with a needle. The microgels were dispersed in a mixture of n-hexane and 1 wt% Span 80. After sedimentation of the microgels, the solution was removed with a syringe and a needle. The microgels were dispersed again in the solution and this step was repeated five times. Subsequently, this process was repeated with the solvents *n*-hexane, isopropanol, and water. The microgels were finally dispersed in water and stored at 4 °C.

Synthesis of TNFα-Antibody-Functionalized Microgels: The microgels were dispersed in 1xPBS (pH 7.4) in an Eppendorf vial. After their sedimentation, PBS was removed with a syringe and a needle. This washing step was repeated five times. Microgels with a corresponding amount of glycidyl groups were dispersed in PBS and TNFα antibody (Amgevita Adalimumab, Amgen, Germany) was added in a ratio of 1:1 to the glycidyl groups. The solution was stirred using a rotating stirrer for 72 h at room temperature to facilitate diffusion and binding of TNFα antibody to the microgels via amine-glycidyl coupling. After sedimentation of the microgels, the microgels were washed five times with fresh PBS as described above. Afterward, remaining glycidyl groups were quenched by reaction with 2-aminoethanol for 2 h at room temperature using a rotating stirrer. The microgels were washed five times with fresh PBS and stored at 4 °C until further use.

Flow Cytometry-Based Binding Studies: GMA-coupled microgels (50 000) (10 eq. GMA) were incubated with fluorescein amine dextran (70 kDa) with a concentration of 1:1 related to the glycidyl groups for different periods of time, ranging from 1 to 16 days at room temperature. In a second experiment, the amount of GMA was varied, ranging from 0.5 to 10 eq., and the microgels were incubated with fluorescein amine dextran (1:1 related to the glycidyl groups) for 4 days. Subsequently, microgels were washed with PBS three times and re-suspended in 150 µL fresh PBS. Flow cytometry analysis was performed at a medium flow rate using the blue λ = 488 nm laser. 10 000 events were recorded for every sample. Measurements were carried out in triplicates and evaluated by use of the FlowJo software (Treestar, OR, USA).

Diffusion Studies and Specific TNFα-Antibody Binding: Diffusion of fluorescently labeled FITC-dextran (20 kDa) inside the microgels was measured via Fluorescence Recovery After Photobleaching (FRAP) technique using Confocal Laser Scanning Microscopy (CLSM) on a Leica TCS SP8 microscope (Leica Microsystems, Germany). The microgels were incubated in PBS with FITC-dextran (1 mg mL^{-1}) via stirring for 48 h at room temperature. FRAP was performed using a 63x dry objective and an excitation wavelength of λ = 488 nm of an Argon-ion laser operating at 80% output power, while the emission was detected at a wavelength of λ = 500–550 nm. A circular region of interest (ROI) with a diameter of 10 µm was placed into the middle of the microgel. A series of images (512 x 512 pixels) was taken with an interval of 1.292 s using a highly attenuated laser beam (1.3% transmission). After recording 30 pre-bleach images, the ROI was bleached at maximum laser intensity (100% transmission) for 1.292 s and another 150 post-bleach images were taken.

The FRAP analysis was based on solving the diffusion equation in the Fourier domain and using that the inverse relative intensity (1-I_{rel}) follows the same differential equation, as the concentration.[39] Transforming the image stack to its spatial Fourier transform, we can collect information from the pixels closest to the center (zero spatial frequency component).

$$I_{rel} = \frac{(I - I_b)}{(I_0 - I_b)} \frac{I_{ref,\,0}}{I_{ref}} \tag{1}$$

$$c\left(q_x,\ q_y,\ t\right) = c_0\left(q_x,\ q_y\right) e^{-4\,\pi\,\left(q_x^2+q_y^2\right)D\,t} \tag{2}$$

An algorithm was written for the analysis in python [https://www.python.org, https://scipy.org] fitting the individual spatial frequency components and the selected components together. This way we could detect if any spatial anisotropy occurred in the data set. This method allows us to obtain the diffusion coefficient independent of the bleaching profile as long as the spatial variation of the original concentration was low in comparison to that of the bleached area.

To determine the diffusion of antibody mimicking dextran, the microgels were incubated in PBS with fluorescein amine dextran (70 kDa) with a concentration of 1:1 related to the glycidyl groups via stirring for 24 h to 96 h at room temperature. Microgels were washed five times with PBS and imaged using CLSM as described above using a 63x dry objective. An excitation wavelength of λ = 488 nm of an Argon-ion laser operating at 25% output power and an emission wavelength of λ = 500–550 nm were employed.

Confocal Fluorescence microscopy and Fluorescence lifetime imaging microscopy (FLIM) was performed using Confocal Laser Scanning Microscopy (CLSM) on a Leica TCS SP8 microscope (Leica Microsystems, Germany). Alexa488 labeled TNFα (custom synthesis TNFα protein conjugated with AlexaFluor 488, Thermo Fisher Scientific, USA) was used as a

© 2023 The Authors. Advanced Healthcare Materials published by Wiley-VCH GmbH

21922659, 2023, 18, Downloaded from https://onlinelibrary.wiley.com/doi/10.1002/adhm.202300695 by Rwth Aachen Hochschulbibliothek, Wiley Online Library on [25/03/2024]. See the Terms and Conditions (https://onlinelibrary.wiley.com/terms-and-conditions) on Wiley Online Library for rules of use; OA articles are governed by the applicable Creative Commons License

donor and Alexa546 labeled TNFα antibody (Amgevita–Adalimumab (Amgen, Germany)), Thermo Fisher Scientific, USA) as acceptor. An excitation wavelength of $\lambda = 488$ nm, as well as a $\lambda = 488$ nm notch filter, was used in front of the detector. The detection band was restricted from 500 to 540 nm with a multiband spectrophotometer. A Single Molecule Detection Hybrid Detector (SMD HyD) in combination with PicoHarp 300 Time-Correlated Single Photon Counting (TCSPC) module has been used to acquire the FLIM decay curves. The decay curves were fitted with a n-Exponential Reconvolution fitting model of SymPhoTime 64 (PicoQuant, Germany) software where the experimental IRF of the instrument was fitted. The IRF was measured in the same excitation-emission conditions of the FRET samples with a solution of fluorescein quenched with KI. For the intensity-based Fluorescence images an HCX PL Fluotar 5x/0.15 dry objective was used and for the FLIM images HC PL APO 63x/1.30 glycerol objective was used to record 512x512 pixels images with a pixel size of 60 nm (64x64 with a pixel size of 500 nm for the donor solution). All measurements were realized at a room temperature of 22.5 °C.

Mechanical Properties of Microgels: The mechanical properties of the microgels with different amounts of GMA were quantified with the high-throughput mechanical screening Nanoindenter Pavone (Optics11Life, Amsterdam, The Netherlands). For each type, a minimum number of 10 microgels were measured. The indentation measurements were performed using a cantilever-based probe with a spherical tip radius of 9.5 µm and a cantilever stiffness of 0.31 N m^{-1}. The indentation speed was set to 1 µm s^{-1} and the indentation depth to 1 µm. The effective Young's modulus E_{eff} (kPa) was determined by fitting the load-indentation curves using the Hertzian model.[40] All measurements were performed in PBS at room temperature.

Quantification of TNFα Antibody in the Microgels: Glycidyl-equipped microgels were incubated with different concentrations of TNFα antibody for 96 h at room temperature. Subsequently, microgels were washed three times with fresh 1xPBS to remove the excess non-bound antibodies. To quantify the amount of TNFα antibody bound to the microgels a CBQCA Protein quantification kit (ThermoFisher Scientific) was used according to the manufacturer's instructions. Briefly, a fixed number of microgels was diluted in a final volume of 135 µL reaction buffer, 5 µL potassium cyanide was added and the reaction was started by the addition of 10 µL ATTO-TAG CBQCA reagent with a working concentration of 2 nM. Both, bovine serum albumin (BSA) and TNFα antibody were used to prepare standard curves as suggested by the manufacturer. Read-out was performed by a BioTek Cytation 3 plate reader (BioTek Instruments GmbH, Bad Friederichshall, Germany) by measuring the fluorescence emission at $\lambda = 550$ nm with excitation at $\lambda = 465$ nm.

TNFα Binding Experiments: Microgels (100 µg = 200 000 microgels mL^{-1}) were incubated with different concentrations of recombinant human TNFα (R&D Systems) for 1 h at 37 °C. Subsequently, samples were centrifuged for 10 min at 3000 rpm and the concentration of TNFα in supernatant was measured by an ELISA kit according to the manufacturer's instructions (R&D Systems).

Cell Experiments (HT29): The human colorectal adenocarcinoma HT29 cells (ATCC HTB38) were cultured in T75 cell culture flasks (Greiner Bio-One GmbH, Frickenhausen, Germany) in RPMI-1640 cell culture medium containing 1% (v/v) penicillin-streptomycin and 10% (v/v) fetal bovine serum. The cells were kept at 37 °C, 5% CO_2, and 95% O_2 in a humidified incubator (Heracell 150i CO_2 incubator, Thermo Fischer Scientific). Cells were seeded in 6 well plates at a density of 500 000 cells per well and allowed to grow to ≈ 80% confluency overnight. Next day, cells were stimulated with TNFα alone, TNFα and microgels, or microgels alone for 24 h at 37 °C. Supernatant was collected and kept at −80 °C until use. Cells were washed with cold PBS to remove the media and harvested in 500 µL cold PBS using a cell scraper. After centrifugation, the supernatant was removed, and the cell pellet was kept at −80 °C.

Protein Isolation and Western Blot (COX II): Proteins were isolated with 1% NP40 lysis buffer containing protease inhibitor, phosphatase inhibitor, and DTT, and the protein concentration was quantified applying a Bradford protein assay (BioRad) according to the manufacturer's instructions. The absorbance was measured using a plate reader (BioTek Instruments GmbH) at a wavelength of $\lambda = 450$ nm. Extracted proteins were separated using SDS-PAGE, transferred to Polyvinylidene difluoride (PVDF) membranes, and incubated with a specific antibody against cyclooxygenase-II (COX II) (Santa Cruz Biotechnology) or an antibody against β-Actin (Sigma) as control. Following washing, a horseradish peroxidase (HRP)-conjugated secondary antibody (Life Technologies) was used, and the desired protein was visualized by use of an enhanced chemiluminescence reagent (GE Healthcare).

IL8 ELISA: The IL8 ELISA (R&D systems, Minneapolis, Germany) was used according to the manufacturer's instructions with slight modifications. 96 well plates were coated with 50 µL of the provided capture antibody, diluted in PBS overnight at 4 °C. Next day, the plates were washed with washing buffer consisting of PBS with 0.05% Tween 20, followed by blocking with 5% BSA in PBS for 1 h at room temperature to avoid unspecific binding. Subsequently, 50 µL of sample or standard, diluted in PBS containing 1% BSA (v/w), were pipetted into the wells and incubated at 4 °C overnight. Next day, samples were removed, the plate was washed and 50 µL of biotin conjugated detection antibody, diluted in PBS with 1% BSA (v/w), was pipetted into each well and incubated for 1 h at room temperature. Plates were washed, and each well was exposed to 50 µL streptavidin HRP for 40 min at room temperature. After washing, 100 µL TMB substrate solution was added per well to induce a color change. After 10 min, the reaction was stopped by adding 50 µL 2N H_2SO_4. Read-out was performed by a BioTek Cytation 3 plate reader (BioTek Instruments GmbH, Bad Friederichshall, Germany) at $\lambda = 450$ nm absorbance.

Macrophage Isolation and Scavenging Experiments: Monocytes were isolated from buffy coats provided by the transfusion medicine department of University Hospital RWTH Aachen. The blood was diluted with PBS in a 1:1 ratio and a Ficoll-based density gradient centrifugation was performed for 1 h at room temperature without the use of the brake as described earlier.[41] The serum of the corresponding donors was heat-inactivated for 1 h at 57 °C.

To isolate monocytes for macrophage culture, the isolated Peripheral Blood Mononuclear Cells (PBMCs) were placed on 2 cm petri dishes at a density of two million cells per mL at a total volume of 2 mL per well. The incubation took place in RPMI cell culture medium containing 5% (v/v) human autologous serum for up to a maximal of 40 min and was carried at 37 °C in a humidified incubator (5% CO_2). During the incubation, monocytes adhered to the petri dish, while leucocytes remained in the supernatant and were removed by subsequent washing with pre-warmed cell culture media. Monocytes were differentiated into macrophages by culturing them for 6 days in RPMI cell culture medium containing 5% (v/v) human autologous serum.

Macrophages were stimulated with cell culture medium alone (negative control), LPS alone, LPS and 100 µg mL^{-1} microgels, or only microgels for 24 h in a humidified incubator at 37 °C. The supernatant was collected and frozen at −80 °C until use. TNFα was measured with a TNFα ELISA kit (R&D systems) as described above. To harvest cells, they were washed by cold PBS and detached by use of a cell scraper.

Statistics: Statistical analysis was performed with Origin 2018, graph pad Prism 8 and ImageJ. Statistical significance was performed using two-way ANOVA with Tukey´s test for multiple comparisons. Asterisks were used to highlighted following two-tailed p-values: ns = non-significant, $^{*}p < 0.05$, $^{**}p < 0.01$, $^{***}p < 0.001$, $^{****}p < 0.0001$.

Supporting Information

Supporting Information is available from the Wiley Online Library or from the author.

Acknowledgements

S.B. and Y.K. contributed equally to this work. This work was funded by the Collaborative Research Center (CRC) on microgels SFB 985 project C3 from DFG (Deutsche Forschungsgemeinschaft) and DFG grant STR 1095/6-1 (to PS). Table of Contents image created with BioRender.com.

© 2023 The Authors. Advanced Healthcare Materials published by Wiley-VCH GmbH

21922659, 2023, 18, Downloaded from https://onlinelibrary.wiley.com/doi/10.1002/adhm.202300695 by Rwth Aachen Hochschulbibliothek, Wiley Online Library on [25/03/2024]. See the Terms and Conditions (https://onlinelibrary.wiley.com/terms-and-conditions) on Wiley Online Library for rules of use; OA articles are governed by the applicable Creative Commons License

After initial online publication, L.D.L. was removed from the affiliation Institute of Organic and Macromolecular Chemistry, Ulm University, on July 17, 2023. Her original association with this affiliation was made in error. The editorial office apologizes for any inconvenience caused.

Open access funding enabled and organized by Projekt DEAL.

Conflict of Interest

The authors declare no conflict of interest.

Data Availability Statement

The data that support the findings of this study are available from the corresponding author upon reasonable request.;

Keywords

antibody, autoimmune disease, inflammation, local therapy, microgels, TNFα scavenging

Received: March 3, 2023
Revised: May 9, 2023
Published online: June 7, 2023

[1] R.-M. Lu, Yu-C Hwang, I-Ju Liu, C.-C. Lee, H.-Z. Tsai, H.-J. Li, H.-C. Wu, *J. Biomed. Sci.* **2020**, *27*, 1.
[2] T. Bongartz, A J. Sutton, M J. Sweeting, I. Buchan, E L. Matteson, V. Montori, *J. Am. Med. Assoc.* **2006**, *295*, 2275.
[3] S. Minozzi, S. Bonovas, T. Lytras, V. Pecoraro, M. González-Lorenzo, A. J. Bastiampillai, E. M. Gabrielli, A. C. Lonati, L. Moja, M. Cinquini, V. Marino, A. Matucci, G. M. Milano, G. Tocci, R. Scarpa, D. Goletti, F. Cantini, *Expert Opin. Drug Saf.* **2016**, *15*, 11.
[4] J W. Myerson, P N. Patel, K M. Rubey, M E. Zamora, M H. Zaleski, N. Habibi, L R. Walsh, Yi-W Lee, D C. Luther, L T. Ferguson, O A. Marcos-Contreras, P M. Glassman, L L. Mazaleuskaya, I. Johnston, E D. Hood, T. Shuvaeva, J. Wu, H.-Y. Zhang, J V. Gregory, R Y. Kiseleva, J. Nong, T. Grosser, C F. Greineder, S. Mitragotri, G S. Worthen, V M. Rotello, J. Lahann, V R. Muzykantov, J S. Brenner, *Nat. Nanotechnol.* **2022**, *17*, 86.
[5] C.-T. Jiang, K-Ge Chen, An Liu, H. Huang, Ya-N Fan, D.-K. Zhao, Q-Ni Ye, H.-B. Zhang, C.-F. Xu, S. Shen, M.-H. Xiong, J.-Z. Du, X.-Z. Yang, J. Wang, *Nat. Commun.* **2021**, *12*, 1359.
[6] A. C. Lima, C. Cunha, A. Carvalho, H. Ferreira, N M. Neves, *ACS Appl. Mater. Interfaces* **2018**, *10*, 13839.
[7] W J. Smith, G. Wang, H. Gaikwad, V P. Vu, E. Groman, D W. A. Bourne, D. Simberg, *ACS Nano* **2018**, *12*, 12523.
[8] M R. Gordon, M. Canakci, L. Li, J. Zhuang, B. Osborne, S. Thayumanavan, *Bioconjug. Chem.* **2015**, *26*, 2198.
[9] M E. Wechsler, R E. Stephenson, A C. Murphy, H F. Oldenkamp, A. Singh, N A. Peppas, *Biomed. Microdevices* **2019**, *21*, 31.
[10] Y. Kittel, A J. C. Kuehne, L. De Laporte, *Adv. Healthcare Mater.* **2022**, *11*, 2101989.
[11] J. Kim, D M. Francis, L F. Sestito, P A. Archer, M P. Manspeaker, M J. O'melia, S N. Thomas, *Nat. Commun.* **2022**, *13*, 1479.
[12] R. Miura, Y. Tahara, S.-I. Sawada, Y. Sasaki, K. Akiyoshi, *Sci. Rep.* **2018**, *8*, 16464.
[13] X. Ma, Ze Zhao, H. Wang, Y. Liu, Y. Xu, J. Zhang, B. Chen, L. Li, Y. Zhao, *Adv. Healthcare Mater.* **2019**, *8*, 1900136.
[14] A. Seyfoori, S. A. Seyyed Ebrahimi, E. Samiei, M. Akbari, *ACS Appl. Mater. Interfaces* **2019**, *11*, 24945.
[15] J. C. Cuggino, E. R. O. Blanco, L. M. Gugliotta, C. I. Alvarez Igarzabal, M. Calderón, *J. Controlled Release* **2019**, *307*, 221.
[16] V K. Switacz, S K. Wypysek, R. Degen, J J. Crassous, M. Spehr, W. Richtering, *Biomacromolecules* **2020**, *21*, 4532.
[17] H. Onishi, Y. Ikeuchi-Takahashi, K. Kawano, Y. Hattori, *Biol. Pharm. Bull.* **2019**, *42*, 1155.
[18] Yu Yuan, Y. Liu, Y. He, B. Zhang, L. Zhao, S. Tian, Q. Wang, S. Chen, Z. Li, S. Liang, G. Hou, B. Liu, Y. Li, *Biomaterials* **2022**, *287*, 121613.
[19] P.-H. Kim, H-Gu Yim, Y.-J. Choi, B.-J. Kang, J. Kim, S-Mo Kwon, B.-S. Kim, N S. Hwang, Je-Y Cho, *J. Controlled Release* **2014**, *187*, 1.
[20] A S. Sonzogni, G. Yealland, M. Kar, S. Wedepohl, L M. Gugliotta, V D. G. Gonzalez, S. Hedtrich, M. Calderón, R J. Minari, *Biomacromolecules* **2018**, *19*, 4607.
[21] S. Singh, N. Drude, L. Blank, P. B. Desai, H. Königs, S. Rütten, K.-J. Langen, M. Möller, F M. Mottaghy, A. Morgenroth, *Adv. Healthcare Mater.* **2021**, *10*, 2100812.
[22] R. Noth, E. Stüber, R. Häsler, S. Nikolaus, T. Kühbacher, J. Hampe, B. Bewig, S. Schreiber, A. Arlt, *J. Crohn's Colitis* **2012**, *6*, 464.
[23] J. S Crowe, K J. Roberts, T M. Carlton, L. Maggiore, M F. Cubitt, S. Clare, K. Harcourt, J. Reckless, T T. Macdonald, K P. Ray, A. Vossenkämper, M R. West, *Sci. Rep.* **2018**, *8*, 4941.
[24] S. Boesveld, A. Jans, D. Rommel, M. Bartneck, M. Möller, L. Elling, C. Trautwein, P. Strnad, A J. C. Kuehne, *ACS Appl. Mater. Interfaces* **2019**, *11*, 25017.
[25] A. Jans, R R. Rosencrantz, A D. Mandić, N. Anwar, S. Boesveld, C. Trautwein, M. Moeller, G. Sellge, L. Elling, A J. C. Kuehne, *Biomacromolecules* **2017**, *18*, 1460.
[26] M E. Pedersen, R M. S. Haegebaert, J. Østergaard, H. Jensen, *Sci. Rep.* **2021**, *11*, 4754.
[27] B G. Amsden, *Macromolecules* **2022**, *55*, 8399.
[28] A J. D. Krüger, J. Köhler, S. Cichosz, J C. Rose, D B. Gehlen, T. Haraszti, M. Möller, L. De Laporte, *Chem. Commun.* **2018**, *54*, 6943.
[29] D. Rommel, M. Mork, S. Vedaraman, C. Bastard, L P. B. Guerzoni, Y. Kittel, R. Vinokur, N. Born, T. Haraszti, L. De Laporte, *Adv. Sci.* **2022**, *9*, 2103554.
[30] J. M. De Rutte, J. Koh, D. Di Carlo, *Adv. Funct. Mater.* **2019**, *29*, 1900071.
[31] J. J. Kim, M. S. Shajib, M. M. Manocha, W. I. Khan, *J. Vis. Exp.* **2012**, e3678.
[32] Y.-J. Liu, Bo Tang, F.-C. Wang, Li Tang, Y.-Y. Lei, Ya Luo, S.-J. Huang, M. Yang, L-Yi Wu, W. Wang, S. Liu, S.-M. Yang, X.-Y. Zhao, *Theranostics* **2020**, *10*, 5225.
[33] K. Truong, M. Ikura, *Curr. Opin. Struct. Biol.* **2001**, *11*, 573.
[34] M Y. Berezin, S. Achilefu, *Chem. Rev.* **2010**, *110*, 2641.
[35] J. H. Chi, Y Ho Kim, D. H. Sohn, G. S. Seo, S. H. Lee, *Biomed. Pharmacother.* **2018**, *108*, 1767.
[36] J.-H. Chi, G. S. Seo, S. H. Lee, *Int. Immunopharmacol.* **2018**, *59*, 134.
[37] M. Bartneck, K.-H. Heffels, Yu Pan, M. Bovi, G. Zwadlo-Klarwasser, J. Groll, *Biomaterials* **2012**, *33*, 4136.
[38] M. Bartneck, F. M. Peters, K. T. Warzecha, M. Bienert, L. Van Bloois, C. Trautwein, T. Lammers, F. Tacke, *Nanomedicine* **2014**, *10*, 1209.
[39] E. Migliorini, P. Horn, T. Haraszti, S V. Wegner, C. Hiepen, P. Knaus, R P. Richter, E. A. Cavalcanti-Adam, *Adv. Biosyst.* **2017**, *1*, 1600041.
[40] D. Xu, T. Harvey, E. Begiristain, C. Domínguez, L. Sánchez-Abella, M. Browne, R B. Cook, *J. Mech. Behav. Biomed. Mater.* **2022**, *133*, 105329.
[41] M. Bartneck, H A. Keul, S. Singh, K. Czaja, J. Bornemann, M. Bockstaller, M. Moeller, G. Zwadlo-Klarwasser, J. Groll, *ACS Nano* **2010**, *4*, 3073.

© 2023 The Authors. Advanced Healthcare Materials published by Wiley-VCH GmbH

21922659, 2023, 18, Downloaded from https://onlinelibrary.wiley.com/doi/10.1002/adhm.202300695 by Rwth Aachen Hochschulbibliothek, Wiley Online Library on [25/03/2024]. See the Terms and Conditions (https://onlinelibrary.wiley.com/terms-and-conditions) on Wiley Online Library for rules of use; OA articles are governed by the applicable Creative Commons License